Smith-Purcell radiation from electrons moving parallel to a grating at oblique incidence to the rulings

O. Haeberlé
Laboratoire de Physique de la Matière Condensée-Ecole Polytechnique, F-91128 Palaiseau, France

P. Rullhusen and J.-M. Salomé
European Commission, Joint Research Centre, Institute for Reference Materials and Measurements, Retieseweg, B 2440 Geel, Belgium

N. Maene
Vlaamse Instelling voor Technologisch Onderzoek, Boeretang 200, B-2400 Mol, Belgium

(Received 15 October 1996)

Smith-Purcell radiation is produced when a charged particle moves parallel and close to a diffraction grating. We extend previous descriptions of the phenomenon by considering a particle moving parallel to the grating surface at an arbitrary angle with respect to the grating rulings. The problem of calculating the emitted radiation intensity is shown to be linked to a special grating problem involving evanescent incident waves and conical diffraction. Conservation relations are derived by applying techniques from electromagnetic grating theory, and Smith-Purcell spectra are calculated for some specific cases of practical interest.
[S1063-651X(97)13403-1]

PACS number(s): 41.60.−m, 42.25.Fx, 42.79.Dj

I. INTRODUCTION

In 1953 Smith and Purcell [1] found the first experimental confirmation for light emission by a fast electron passing close to a periodic structure. The Smith-Purcell (SP) effect belongs to the general class of radiation effects induced by electrons interacting with a medium. These types of radiation can be modeled considering radiation from the medium, induced by the electric charge of the electron, or considering refraction, reflection, and diffraction of evanescent waves associated with the electromagnetic field of the electron. The Cherenkov radiation [2–4] is probably the most familiar of these phenomena. It is produced when a charged particle moves inside a medium of index of refraction n at a velocity $v>c/n$, c being the vacuum speed of light, as indicated in Fig. 1(a). The effect is very similar to the production of acoustical Mach waves produced by objects moving at supersonic velocities. Closely related to the Cherenkov effect is the production of transition radiation [5,6] when the electron crosses a thin foil [c.f. Fig. 1(b)]. The diffraction of evanescent waves by an obstacle as indicated in Fig. 1(c) leads to the so-called diffraction radiation [7,8], of which the SP effect, depicted in Fig. 1(d), could be considered as a special case for periodical structures.

In 1961, Toraldo di Francia [9] applied the concept of diffraction of evanescent waves to explain the SP effect from shallow grating profiles. Several methods have been proposed [10] in optics to find the reflection efficiency of a grating from the Maxwell equations and the boundary conditions. The applicability of these different methods to the calculation of SP radiation has been discussed in our previous paper [11], to which we will refer as I in the following.

After the discovery of the SP effect it soon became clear that it might be used as radiation source in the millimeter to visible range for which tunable sources were hardly or not available at that time. Several experiments [12–15] have been carried out using electrons in the 50–200-keV energy range, and recently [16–19] also at MeV energies. Considerable efforts have been undertaken [20–23] to build free-electron lasers based on the SP effect in an Orotron configuration [24].

The experiments and theoretical approaches have been restricted until now to electron trajectories perpendicular to the rulings of the grating. For electron trajectories at an angle $\Psi\neq 0°$ to the rulings, it can be expected [1,25] that the apparent grating period $D/\cos\Psi$ would lead to a modified wavelength, thus offering the possibility of fine tuning the SP radiation. In optics it is known [10] that the spectral-angular distribution is strongly modified in conical diffraction geometry. The purpose of our article is to study this effect in the case of SP radiation, extending our previous investigations [11] to electron trajectories at oblique incidence, although still parallel to the grating surface. The formalism does not apply to electron trajectories which are not parallel to the grating surface, as discussed, e.g., in [12,13,25,26].

II. GENERAL FORMALISM

In Fig. 2 we give a schematical description of the experiment and the relevant geometrical quantities. The electron moves in vacuum at a distance z_0 parallel to the surface of a grating which is assumed to be electrically perfect conducting. The top of the grating is in the (x,y) plane and the grating profile is described by a periodic function $z=f(x)=f(x+D)$ with the direction of the rulings parallel to the y axis. By convention, the vector $\mathbf{n}$ normal to the surface is pointing inside the grating. The electron moves at an angle Ψ to the x axis with constant velocity $\mathbf{v}=v(\hat{\mathbf{i}}_x\cos\Psi+\hat{\mathbf{i}}_y\sin\Psi)$, with $\hat{\mathbf{i}}_x$, $\hat{\mathbf{i}}_y$, and $\hat{\mathbf{i}}_z$ being unit vectors in the x, y, and z directions, respectively. In our formalism we follow closely the notation of van den Berg [27], also used in I. The field

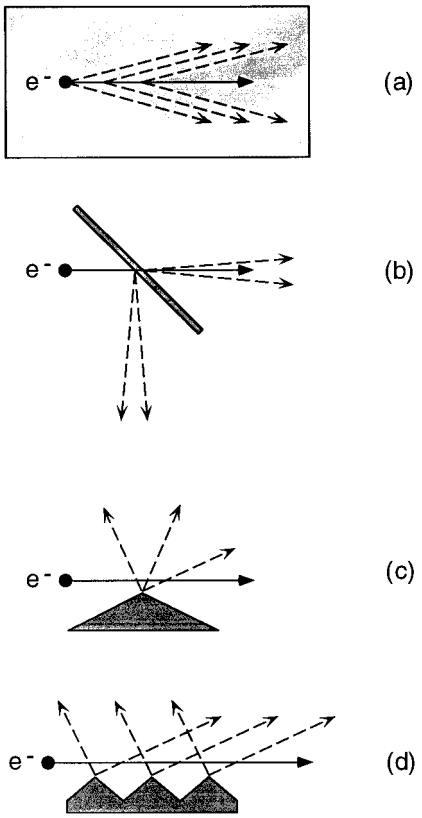

FIG. 1. Radiative processes by relativistic electrons interacting with a medium. (a) Cherenkov radiation produced when the electron moves at constant speed $v>c/n$ in a medium of index of refraction n. (b) Transition radiation produced when the electron traverses a thin foil. (c) Diffraction radiation generated when the electron passes close to an obstacle. (d) Smith-Purcell radiation when the electron passes close to a periodic structure.

vectors $\mathbf{E}^i(x,y,z,t)$ and $\mathbf{H}^i(x,y,z,t)$ of the Coulomb field of the electron can be expanded in terms of Fourier integrals.

$$\mathbf{E}^i(x,y,z,t)=(2\pi)^{-2}\int_{-\infty}^{+\infty}d\omega\int_{-\infty}^{-\infty}d\beta\,\mathscr{E}^i(x,z;\beta,\omega)\times\exp(i\beta y-i\omega t), \tag{1}$$

$$\mathbf{H}^i(x,y,z,t)=(2\pi)^{-2}\int_{-\infty}^{+\infty}d\omega\int_{-\infty}^{\infty}d\beta.\mathscr{H}^i(x,z;\beta,\omega)\times\exp(i\beta y-i\omega t), \tag{2}$$

Since the fields are real and only positive values of ω are considered, the previous expressions are rewritten as

$$\mathbf{E}^i(x,y,z,t)=(2\pi^2)^{-1}\mathrm{Re}\left[\int_0^{+\infty}d\omega\int_{-\infty}^{\infty}d\beta\,\mathscr{E}^i(x,z;\beta,\omega)\times\exp(i\beta y-i\omega t)\right], \tag{3}$$

$$\mathbf{H}^i(x,y,z,t)=(2\pi^2)^{-1}\mathrm{Re}\left[\int_0^{+\infty}d\omega\int_{-\infty}^{\infty}d\beta.\mathscr{H}^i(x,z;\beta,\omega)\times\exp(i\beta y-i\omega t)\right]. \tag{4}$$

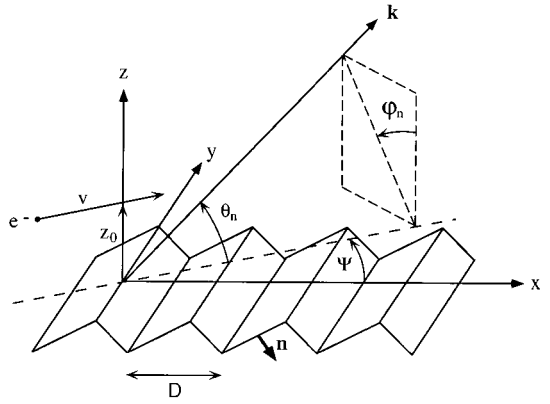

FIG. 2. Geometry of a Smith-Purcell experiment at oblique incidence.

These Fourier components satisfy the Maxwell equations, which take the following form:

$$(\boldsymbol{\nabla}+i\beta\hat{\mathbf{i}}_y)\times.\mathscr{H}^i+i\omega\varepsilon_0\mathscr{E}^i=\mathscr{J}, \tag{5}$$

$$(\boldsymbol{\nabla}+i\beta\hat{\mathbf{i}}_y)\times\mathscr{E}^i-i\omega\mu_0.\mathscr{H}^i=0, \tag{6}$$

with $\boldsymbol{\nabla}=\partial_x\hat{\mathbf{i}}_x+\partial_z\hat{\mathbf{i}}_z$ and $\mathscr{J}=\mathscr{J}(x,z;\beta,\omega)$ being the Fourier transform of the current density. The current density due to the electron charge $q=-e$ moving with velocity $\mathbf{v}$ is given by

$$\mathbf{J}(x,y,z,t)=q\mathbf{v}\delta(x-vt\,\cos\Psi,y-vt\,\sin\Psi,z-z_0), \tag{7}$$

and the corresponding Fourier transform is obtained as

$$\mathscr{J}(x,z;\beta,\omega)=q\,\delta(z-z_0)\{\hat{\mathbf{i}}_x+\hat{\mathbf{i}}_y\,\tan\Psi\}\times\exp\left[i(\omega-\beta v\,\sin\Psi)\,\frac{x}{v\,\cos\Psi}\right]. \tag{8}$$

As for SP radiation produced by electrons moving perpendicular to the grating rulings, the Maxwell equations allow us to write the x and z components of the Fourier field vectors $\mathscr{E}^i$ and $\mathscr{H}^i$ as functions of their y components E_y^i and H_y^i which satisfy the two-dimensional Helmholtz equations

$$(\partial_x^2+\partial_z^2)E_y^i+(k^2-\beta^2)E_y^i=-i\omega\mu_0J_y+\frac{\beta}{\omega\varepsilon_0}(\partial_xJ_x+i\beta J_y), \tag{9}$$

$$(\partial_x^2+\partial_z^2)H_y^i+(k^2-\beta^2)H_y^i=-\partial_zJ_x, \tag{10}$$

where $k=\omega/c$, and c is the vacuum speed of light. The solutions of these equations are given by

$$E_y^i(x,z;\beta,\omega)=\frac{q}{2}\left(\frac{\mu_0}{\varepsilon_0}\right)^{1/2}\left[\frac{\beta c/v-k\,\sin\Psi}{\gamma_0\,\cos\Psi}\right]\times\exp(i\alpha_0x+i\gamma_0|z-z_0|) \tag{11}$$

$$H_y^i(x,z;\beta,\omega)=-\frac{q}{2}\,\mathrm{sgn}(z-z_0)\exp(i\alpha_0x+i\gamma_0|z-z_0|), \tag{12}$$

in which $\alpha_0=\omega/(v\cos\Psi)-\beta\tan\Psi$ and $\gamma_0=i(\alpha_0^2+\beta^2-k^2)^{1/2}$ with $(\alpha_0^2+\beta^2-k^2)^{1/2}>0$. As a consequence of $v<c$ it can be shown that $\alpha_0^2+\beta^2>k^2$. Therefore, γ_0 is always imaginary and nonzero, which means that the electromagnetic field generated by the moving electron is represented by a set of evanescent plane waves exponentially decaying in the direction away from the electron trajectory (cf. I). In the absence of any perturbing device the free electron moving in empty space does not radiate. However, when the electron moves close to a grating the evanescent waves are diffracted by the grating and some of these diffracted waves may be propagative, constituting the SP radiation.

The reflected fields are given by $\mathbf{E}^r=\mathbf{E}-\mathbf{E}^i$ and $\mathbf{H}^r=\mathbf{H}-\mathbf{H}^i$, with $\mathbf{E}(x,y,z,t)$ and $\mathbf{H}(x,y,z,t)$ being the total fields above the grating surface. These reflected fields can also be expanded as Fourier integrals with the Fourier transforms $\mathscr{E}^r$ and $\mathscr{H}^r$ satisfying the source-free Maxwell equations

$$(\boldsymbol{\nabla}+i\beta\hat{\mathbf{i}}_y)\times\mathscr{H}^r+i\omega\varepsilon_0\mathscr{E}^r=0, \tag{13}$$

$$(\boldsymbol{\nabla}+i\beta\hat{\mathbf{i}}_y)\times\mathscr{E}^r-i\omega\mu_0\mathscr{H}^r=0. \tag{14}$$

The boundary condition for a perfectly conducting surface is $\hat{\mathbf{n}}\times\mathbf{E}=\mathbf{0}$, in which $\hat{\mathbf{n}}$ is the unit vector normal to the surface (cf. Fig. 2), and $\mathbf{E}$ the total electric field. As for the incident field, from the Maxwell equations one can show that the x and z components of the electric and magnetic fields can be expressed in terms of the y components E_y^r and H_y^r. It can be shown from the boundary condition that there is no coupling between E_y and H_y and, therefore, the three-dimensional vectorial problem can be separated into two scalar problems of two dimensions called the two fundamental cases of polarization (viz., the E and H polarizations). In the E-polarization case, where $E_y^r\neq0$ and $H_y^r=0$, one obtains the Helmholtz equation for the reflected field,

$$(\partial_x^2+\partial_z^2)E_y^r+(k^2-\beta^2)E_y^r=0, \tag{15}$$

with the boundary condition $E_y=0$ for the total field on the surface. In the H-polarization case, where $E_y^r=0$ and $H_y^r\neq0$, one obtains

$$(\partial_x^2+\partial_z^2)H_y^r+(k^2-\beta^2)H_y^r=0, \tag{16}$$

with the boundary condition $\hat{\mathbf{n}}\cdot\boldsymbol{\nabla}H_y=0$ on the surface. The observable reflected field must be given by outgoing waves propagating away from the grating and bounded for $z\to\infty$. This is called the ''radiation condition'' [24]. Let $E_y^r(x,z;\beta,\omega)$ and $H_y^r(x,z;\beta,\omega)$ be solutions for the reflected fields. Since $\exp(-i\alpha_0x)E_y^i$, $\exp(-i\alpha_0x)H_y^i$, and the boundary conditions are periodic in x, the quantities $\exp(-i\alpha_0x)E_y^r$ and $\exp(-i\alpha_0x)H_y^r$ will also be periodic in x and can be represented as Fourier series. Therefore, for E_y^r and H_y^r, one obtains

$$E_y^r(x,z;\beta,\omega)=\sum_{n=-\infty}^{\infty}E_{y,n}^r(z;\beta,\omega)\exp(i\alpha_nx), \tag{17}$$

$$H_y^r(x,z;\beta,\omega)=\sum_{n=-\infty}^{\infty}H_{y,n}^r(z;\beta,\omega)\exp(i\alpha_nx), \tag{18}$$

with $\alpha_n=\alpha_0+2\pi n/D$. These expressions are inserted into the Helmholtz equations. For $0<z<\infty$ the orthogonality of the functions $\exp(i\alpha_nx)$ on any interval $x_1\leqslant x\leqslant x_1+D$ gives

$$\partial_z^2E_{y,n}^r(z;\beta,\omega)+\gamma_n^2E_{y,n}^r(z;\beta,\omega)=0, \tag{19}$$

$$\partial_z^2H_{y,n}^r(z;\beta,\omega)+\gamma_n^2H_{y,n}^r(z;\beta,\omega)=0, \tag{20}$$

with $\gamma_n^2=k^2-\beta^2-\alpha_n^2$. Above the grating, the solutions of these equations are given by

$$E_{y,n}^r(z;\beta,\omega)=E_{y,n}^r(\beta,\omega)\exp(i\gamma_nz), \tag{21}$$

$$H_{y,n}^r(z;\beta,\omega)=H_{y,n}^r(\beta,\omega)\exp(i\gamma_nz), \tag{22}$$

with $\mathrm{Re}(\gamma_n)\geqslant0$ and $\mathrm{Im}(\gamma_n)\geqslant0$. Solutions involving $\exp(-i\gamma_nz)$ are rejected because for $\gamma_n^2\geqslant0$ they would represent waves propagating into the grating, and for $\gamma_n^2<0$ and $z\to\infty$ the amplitudes would become infinite. Using Eqs. (17)–(22) the diffracted field above the grating can be written as an infinite sum of outgoing propagative or evanescent plane waves:

$$E_y^r(x,z;\beta,\omega)=\sum_{n=-\infty}^{\infty}E_{y,n}^r(\beta,\omega)\exp(i\alpha_nx+i\gamma_nz), \tag{23}$$

$$H_y^r(x,z;\beta,\omega)=\sum_{n=-\infty}^{\infty}H_{y,n}^r(\beta,\omega)\exp(i\alpha_nx+i\gamma_nz). \tag{24}$$

It is worth mentioning that the so-called ''Rayleigh expansions'' (23) and (24) are valid only for $z\geqslant0$ because the differential equation system (19) and (20) is only valid outside the grooves. They are valid, however, independent of the grating profile, even for nonanalytic profiles like, e.g., semi-infinite screens of vanishing thickness, and independent of the surface material. In order to calculate the diffracted fields, the coefficients $E_{y,n}^r$ and $H_{y,n}^r$ in the Rayleigh expansions for the fields outside the grooves have to be found. For a description of the methods used to solve this so-called ''grating problem'' see, e.g., the book by Petit [10].

III. RADIATION FACTORS

As stated above, the SP radiation is the sum of all propagative waves diffracted from the grating [i.e., all waves with $\mathrm{Im}(\gamma_n)=0$]. This requires that $\alpha_n^2+\beta^2\leqslant k^2$, which restricts β to $-k\leqslant\beta\leqslant k$. In this case we have $\alpha_0>0$ and therefore $\alpha_n^2>\alpha_0^2$ for positive n. Since $\alpha_0^2+\beta^2>k^2$ we would obtain $\alpha_n^2+\beta^2>k^2$, which is a contradiction. As a consequence there are no solutions for propagative waves with positive orders n. For the outgoing wave it is most natural to introduce the observation angles (θ,φ) as depicted in Fig. 2, which are closely related to the angles (η,ζ) used in I for electron trajectories perpendicular to the rulings. In the treatment of conical diffraction, however, it is more convenient to introduce a different set of observation angles (Θ,Φ) as depicted in Fig. 3 and defined by

$$\alpha_n=-k\sin\Theta_n\sin\Phi_n, \tag{25}$$

$$\beta=k\cos\Phi_n, \tag{26}$$

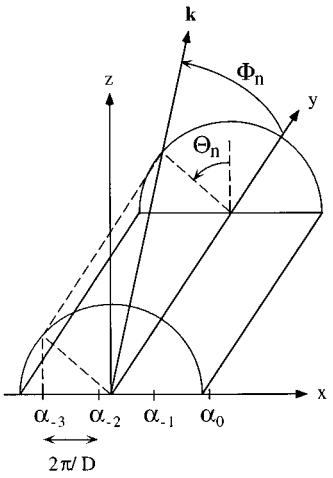

FIG. 3. Construction of the emerging waves produced by the diffraction of an incident wave with parameters α_0, β, and γ_0. The waves of different orders of diffraction n are located on a cone of aperture Φ_n centered around the y axis, with $\cos\Phi_n=\beta/k$.

$$\gamma_n=k\ \cos\Theta_n\sin\Phi_n\,. \tag{27}$$

For an incident wave with parameters α_0, β, and γ_0, the corresponding propagative diffracted waves with parameters α_n, β, and γ_n are located on a cone. Figure 3 illustrates the construction of the emerging waves for a diffraction order n. When a conical diffraction mounting is used in spectroscopy, the parameters α_0, β, and γ_0 of the incident wave are fixed by the experiment. In contrast, in the SP case for a fixed value of k all values $|\beta|\leqslant k$ are allowed, with one cone of associated diffraction orders for each value of β. From Eqs. (25) and (26), for the wavelength $\lambda=2\pi/k$ we obtain

$$-n\lambda=\frac{D}{\cos\Psi}\left(\frac{c}{v}-\sin\Psi\ \cos\Phi_n+\cos\Psi\ \sin\Theta_n\sin\Phi_n\right). \tag{28}$$

In the reference system of Fig. 2, the angles of observation (θ,φ) for a specific diffraction order n are given by

$$\alpha_n=k(\cos\Psi\ \cos\theta_n-\sin\Psi\ \sin\theta_n\sin\varphi_n), \tag{29}$$

$$\beta=k(\sin\Psi\ \cos\theta_n+\cos\Psi\ \sin\theta_n\sin\varphi_n), \tag{30}$$

$$\gamma_n=k\ \sin\theta_n\cos\varphi_n\,, \tag{31}$$

and the diffraction law (28) becomes

$$-n\lambda=\frac{D}{\cos\Psi}\left(\frac{c}{v}-\cos\theta_n\right). \tag{32}$$

For $\Psi=0$ the well-known SP diffraction law is obtained. From Eqs. (29)–(32) several peculiarities of SP spectra can be deduced using the same arguments as in I: (i) For a certain wavelength λ the maximum observable diffraction order n is given for $\theta_n=180°$,

$$|n_{\max}|=\frac{D}{\lambda}\,\frac{1+c/v}{\cos\Psi}, \tag{33}$$

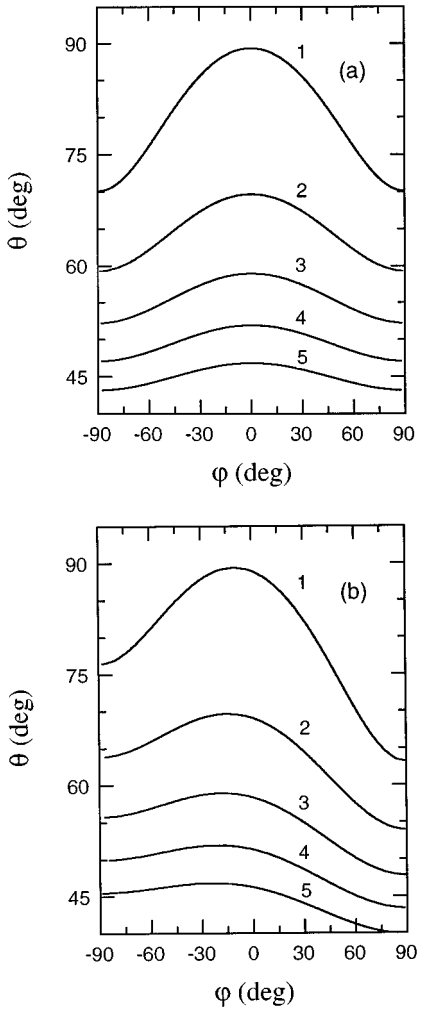

FIG. 4. Positions (θ_w,φ_w) of the first five Wood-Rayleigh anomalies for SP radiation produced by 2-MeV electrons. (a) $\Psi=0°$; (b) $\Psi=10°$.

(ii) Observing SP radiation in first order $n=-1$, the so-called ''Wood-Rayleigh anomalies'' [28,29] are expected [30] to be seen in the spectra at angles θ_w and corresponding wavelengths λ such that the maximum observable orders $n_{\max}=-2,-3,...$ satisfy Eq. (33). For $\Psi=0$ and $\varphi=0$ this leads to a simple formula [11] which allows us to predict the angles where these anomalies are located. In the more general cases $\Psi\neq0$ and $\varphi\neq0$, a somewhat more complicated quadratic expression in $x=\sin\theta_w\sin\varphi_w$ and $y=\cos\theta_w$ is obtained, which yields θ_w as a function of φ_w:

$$Ay^2-2By+C=0, \tag{34}$$

with

$$A=1+2m+(m/\cos\Psi)^2, \tag{35}$$

$$B=m(x\ \tan\Psi+c/v)+(m/\cos\Psi)^2c/v, \tag{36}$$

$$C=x^2+2m(c/v)x\ \tan\Psi+(m/\cos\Psi)^2(c/v)^2-1, \tag{37}$$

and $m=|n_{\max}|-1=1,2,3,...$. In Fig. 4 we show two examples calculated for 2-MeV electrons incident on a grating at (a) $\Psi=0°$ and (b) $\Psi=10°$. As can be seen from Fig. 4(b), the

Wood-Rayleigh anomalies for incidence angles $\Psi \neq 0$ are not distributed symmetrically to the observation plane $\varphi=0$ perpendicular to the grating.

The power density (i.e., energy per unit area and per unit time) radiated in spectral order n is given by the real part of the Poynting vector:

$$\frac{1}{2}\,\mathscr{E}_n^r \times .\mathscr{H}_n^{r*} = \frac{1}{2}\,\frac{\omega}{k^2-\beta^2}\,(\varepsilon_0 |E_{y,n}^r|^2 + \mu_0 |H_{y,n}^r|^2)\mathbf{k}_n, \quad (38)$$

with $\mathbf{k}_n=(\alpha_n,\beta,\gamma_n)$ being the wave vector of the propagative diffracted wave. When the electron traverses one period D of the grating the total radiated energy $W=\Sigma W_n$ of all spectral orders n is equal to the work needed to move the electron against the action of the reflected field [27];

$$W=\sum_n W_n = \frac{D}{\pi^2}\int_0^\infty d\omega \int_{-\infty}^{\infty} d\beta \sum_n \left(\tfrac{1}{2}\mathscr{E}_n^r \times .\mathscr{H}_n^{r*}\right)\cdot \hat{\mathbf{i}}_z, \quad (39)$$

with the summation taken over all spectral orders n for which γ_n is real. In analogy to the case when $\Psi=0°$ [11,27], we introduce a modified radiation factor $R_n(\theta,\varphi,\Psi)$ with

$$|R_n(\theta,\varphi,\Psi)|^2 = \frac{4}{e^2(1-\Delta^2)}\left\{\frac{\varepsilon_0}{\mu_0}\left|E_{y,n}^r\right|^2 + \left|H_{y,n}^r\right|^2\right\} \times \exp(2|\gamma_0|z_0), \quad (40)$$

$$\Delta = \frac{\beta}{k} = \cos\theta\,\sin\Psi + \sin\theta\,\sin\varphi\,\cos\Psi. \quad (41)$$

As in the case where $\Psi=0°$, the exponential decay of the radiation factor with increasing z_0 is compensated for in Eq. (40) introducing an additional factor $\exp(2|\gamma_0|z_0)$.

The absence of coupling between the fields shows that the methods used to solve the grating problem for SP radiation at $\Psi=0°$ can also be used to calculate SP radiation at oblique incidence, provided that the new expressions for the incoming fields, the dispersion relation, and the radiation factors are used. With the definition (40) for the radiation factors, from Eqs. (38) and (39) for the energy radiated in spectral order n we finally obtain

$$W_n = \frac{e^2D^2}{2|n|\varepsilon_0}\int_0^\pi \int_{-\pi/2}^{\pi/2} \frac{\sin^2\theta\,\cos^2\varphi}{\lambda^3}\,|R_n(\theta,\varphi,\Psi)|^2 \times \exp(-z_0/h_{\rm int}^n)\sin\theta d\theta\, d\varphi, \quad (42)$$

in which λ is a function of θ according to Eq. (32), and introducing an interaction range

$$h_{\rm int}^n = \frac{1}{2|\gamma_0|} = \frac{\lambda}{4\pi}\cos\Psi[(c/v-\Delta\,\sin\Psi)^2 + (\Delta^2-1)\cos^2\Psi]^{-1/2}, \quad (43)$$

which agrees with the previously found [11,27] expression when $\Psi=0°$. The power emitted in spectral order n into a solid angle $d\Omega$ in direction (θ,φ) by one electron per second traversing one period D of the grating at a distance z_0 is then given by [31]

$$\left(\frac{dP}{d\Omega}\right)_n = \frac{e^2D^2}{2\varepsilon_0|n|\lambda^3}\,|R_n(\theta,\varphi,\Psi)|^2\sin^2\theta\,\cos^2\varphi \times \exp(-z_0/h_{\rm int}^n). \quad (44)$$

Since the radiation factor defined in Eq. (40) does not depend on the distance z_0 of the electron trajectory to the grating surface the power of SP radiation emitted by an electron beam is obtained integrating Eq. (44) over the beam profile [11,14] and multiplying by the total number of grooves of the grating. When a pulsed beam is used and the wavelength of the emitted photons is comparable to the bunch length, coherence effects may have to be taken into account [17–19]. Such coherent effects will not be considered in the following.

Rotating the grating around the z axis has two main effects. First, the apparent grating period seen by the moving electron changes, and the emitted radiation wavelength changes according to Eq. (32), offering a practical way for fine tuning the SP radiation without changing the electron energy nor the direction of observation. Second, the polarization of the SP radiation changes because the incoming electromagnetic field [Eqs. (11) and (12)] is a function of the angle Ψ. For $\Psi=0°$ the radiation emitted in the x-z plane is purely H polarized. In contrast, when $\Psi\neq 0°$, purely H-polarized radiation is emitted in a cone around the y-axis defined by $\cos\Phi_n=(v/c)\sin\Psi$ (cf. Fig. 3). For $\Psi\neq 0°$ the SP emission diagram is not symmetrical with respect to the x-y plane, nor to the plane containing the electron beam trajectory $\varphi_n=0$.

IV. CONSERVATION RELATIONS

In the ''classical'' grating problem, a grating is illuminated by an incident plane wave, and a first test to check the validity of the calculations is to apply the energy conservation theorem, i.e., the sum of the energies of the diffracted propagative orders has to be equal to the energy of the incident wave. In the special case of Smith-Purcell radiation the energy conservation law is valid for the system electron plus electromagnetic field. For the Rayleigh coefficients, modified conservation relations can be established. They are similar to those for Smith-Purcell radiation at perpendicular incidence, a demonstration of which can be found in [27], to which the interested reader is referred for further details. Let S be a periodic perfectly conducting surface with period D, described by $z=f(x)$, and U and U' two functions satisfying

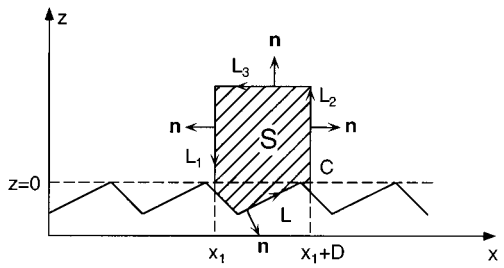

FIG. 5. Domain to which Green's theorem is applied in the derivation of Eq. (49).

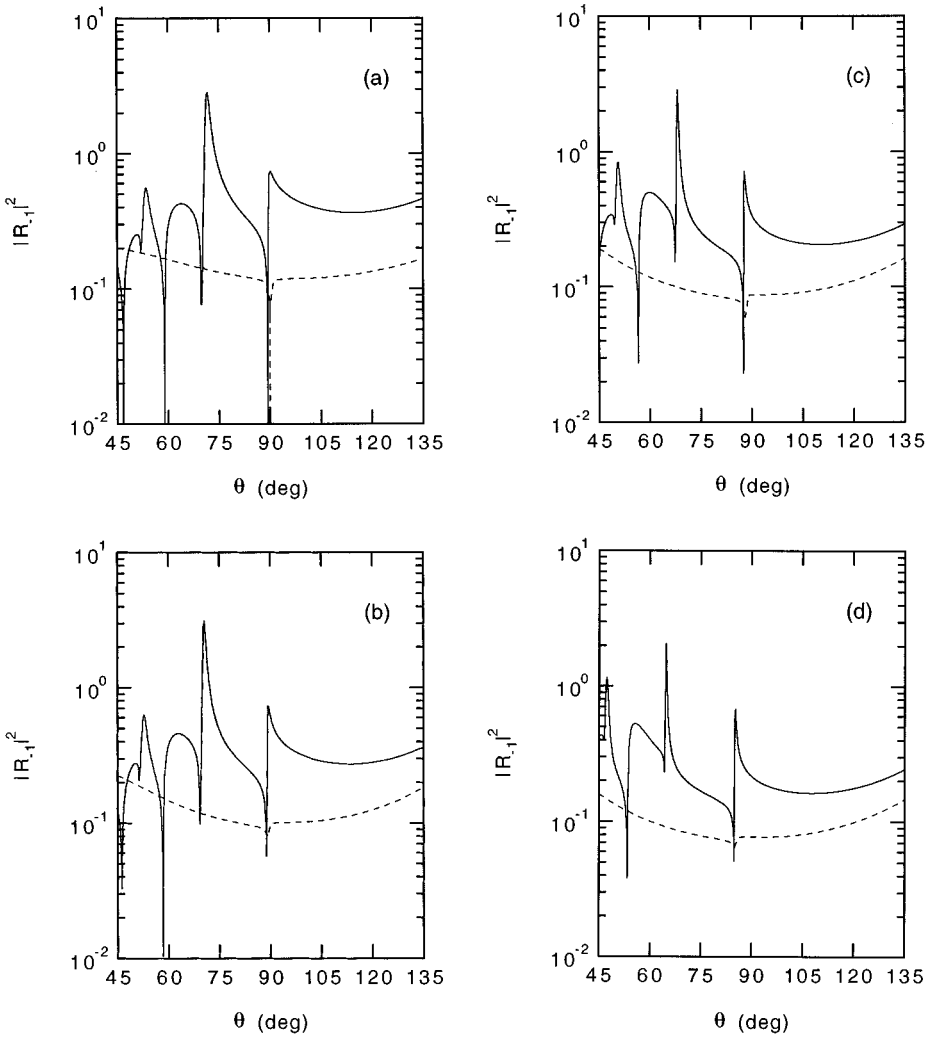

FIG. 6. Radiation factors $|R_{-1}|^2$ in first order at $\varphi=0°$ for several tilting angles Ψ. Solid lines: lamellar grating with $a/D=0.1$ and $h/D=0.5$, and an electron energy of 2 MeV. Dashed lines: sinusoidal grating with $a/D=0.1$, and an electron energy of 10 MeV. (a) $\Psi=0°$, (b) $\Psi=10°$, (c) $\Psi=20°$, and (d) $\Psi=30°$.

the Helmholtz equation above the surface (i.e., for all $z\geqslant 0$). Then we have

$$\nabla^2 U + k^2 U = 0, \tag{45}$$

$$\nabla^2 U' + k^2 U' = 0, \tag{46}$$

and, as a consequence,

$$U'\nabla^2 U - U\nabla^2 U' = 0. \tag{47}$$

Applying the two-dimensional Green's theorem to a domain S inside the closed contour C described in Fig. 5, the following equation is obtained:

$$\int\int_S (U'\boldsymbol{\nabla}^2 U - U\boldsymbol{\nabla}^2 U')\,dS = \oint_C \{U(\mathbf{n}\cdot\boldsymbol{\nabla}U') - U'(\mathbf{n}\cdot\boldsymbol{\nabla}U)\}\,ds = 0. \tag{48}$$

U and U' will be identified later with E_y, E_y^* or H_y, H_y^* for the cases of E polarization or H polarization, respectively (A^* denoting the complex conjugate of A). In the first case U and U' satisfy the Dirichlet boundary condition (i.e., $U=0$, $U'=0$) and in the second case they satisfy the Neumann boundary condition (i.e., $\mathbf{n}\cdot\boldsymbol{\nabla}U=0$, $\mathbf{n}\cdot\boldsymbol{\nabla}U'=0$). Taking into account these boundary conditions, the contribution from L to the contour integral in Eq. (48) vanishes. Since $\exp(-i\alpha_0 x)U$ and $\exp(-i\alpha_0 x)U'$ are periodic in x the contributions from L_1 and L_2 to the contour integral (48) cancel. As a consequence, only the contribution from L_3 remains in the contour integration, and we obtain

$$\int_{x_1}^{x_1+D} \{U\partial_z U' - U'\partial_z U\}\,dx = 0 \tag{49}$$

for any $z\geqslant 0$ above the rulings. Applying Eq. (49) to the couples E_y, E_y^* and H_y, H_y^* in the region $0\leqslant z<z_0$, one obtains the relations

$$\sum_{\text{real } \gamma_n} |E^r_{y,n}|^2 \gamma_n = 9K\ \mathrm{Re}[E^r_{y,0}\exp(i\gamma_0 z_0)], \tag{50}$$

$$\sum_{\text{real } \gamma_n} |H^r_{y,n}|^2 \gamma_n = -q\ \mathrm{Re}[H^r_{y,0}\gamma_0\exp(i\gamma_0 z_0)], \tag{51}$$

in which

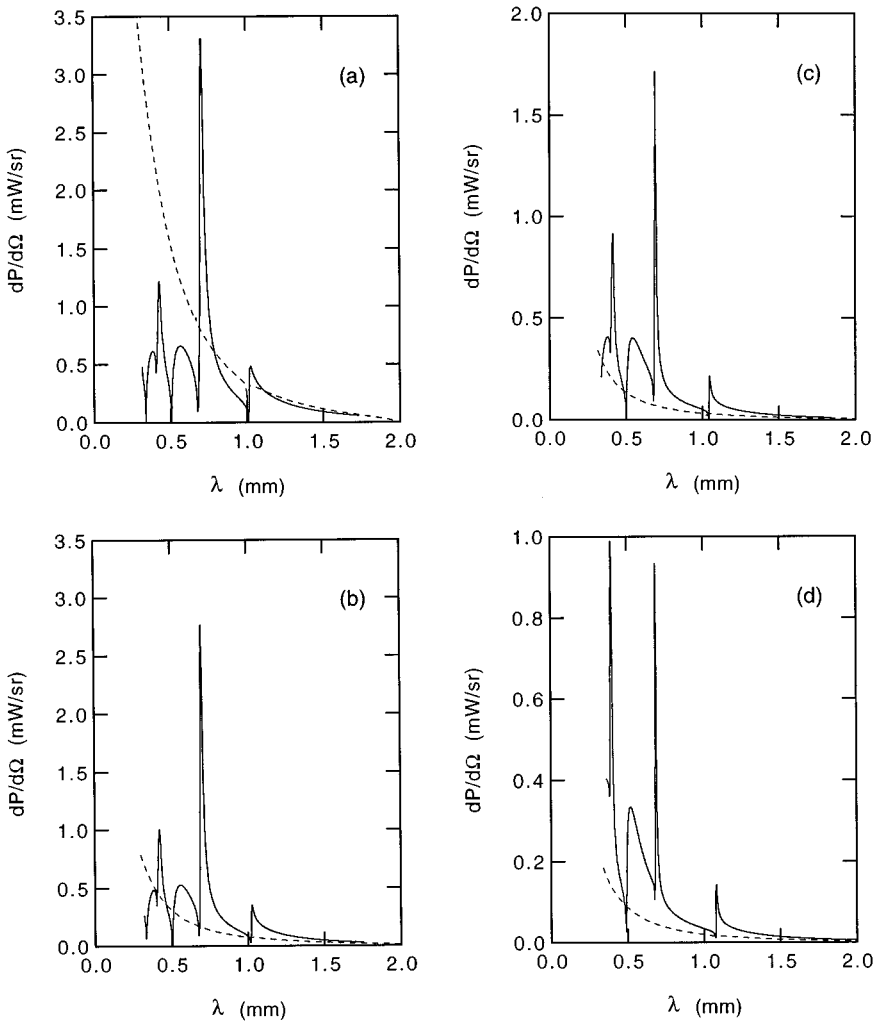

FIG. 7. SP spectra in first order at $\varphi=0°$ and for several tilting angles Ψ in the angular range $45°\leqslant\theta\leqslant135°$. See text for beam parameters. Solid lines: lamellar grating with $a/D=0.1$ and $h/D=0.5$, and an electron energy of 2 MeV. Dashed lines: sinusoidal grating with $a/D=0.1$ and an electron energy of 10 MeV. (a) $\Psi=0°$, (b) $\Psi=10°$, (c) $\Psi=20°$, and (d) $\Psi=30°$.

$$K=\left(\frac{\mu_0}{\varepsilon_0}\right)^{1/2}\left[\frac{\beta c/v-k\,\sin\Psi}{\gamma_0\cos\Psi}\right]. \tag{52}$$

The summations are taken over all propagative orders. Relations (50) and (51) are equivalent to the energy balance criterion [10] in spectroscopy, and can be used to test the validity of the results.

V. RESULTS

In Figs. 6(a)–6(d) we show radiation factors $|R_{-1}|^2$ calculated for the first diffracted order as a function of the tilting angle Ψ and the observation angle θ, but at fixed angle $\varphi=0°$. Solid lines are for an electron energy of 2 MeV, and the grating has a rectangular profile with $h/D=0.1$ and $a/D=0.5$, as used before in I. We used the modal expansion formalism [32,33], which is suitable for this type of grating. The dashed curves are for a sinusoidal grating with $h/D=0.1$ and an electron energy of 10 MeV, as also used before in I. For this type of shallow gratings the Rayleigh method [34] has proven to be correct [35]. In both cases, numerical implementation of the grating problem requires a truncation of the infinite Rayleigh expansions. The order of truncation was increased until convergence had been achieved, and the accuracy of the computation was checked using the conservation relations (50) and (51). In order to arrive at realistic power spectra, we integrated Eq. (44) over a beam profile represented by a symmetrical two-dimensional Gaussian distribution with $\sigma_y=\sigma_z=1.5$ mm. The beam axis is at a distance $z_0=1.5$ mm above the grating, which is shielded against electrons at $z<0$. The grating period is $D=1$ mm, the total length is 10 cm and the (peak) current is 10 Å. Neither an angular divergence of the electron beam nor coherence effects have been taken into consideration. The beam parameters are the same parameters as used in I, and have not been optimized to obtain maximum emission. Figures 7(a)–7(d) show the spectra obtained from the radiation factors depicted in Fig. 6. The results are presented as functions of the wavelength using Eq. (32). In the forward direction the spectra are characterized by strong variations near Wood-Rayleigh anomalies for the lamellar grating. The curves for the sinusoidal grating are rather smooth, except in a very narrow angular range near a Wood-Rayleigh anomaly. In order to maximize the observed intensity when using lamellar gratings, for a certain observation angle θ the corresponding optimum angle φ has to be chosen, usually close and above φ_w as given in Fig. 4. For both types of gratings we observe a decrease of the radiated emission with increasing angle Ψ. This could limit the interest of using Smith-Purcell radiation at oblique incidence to produce tunable radiation. In Fig. 8 we show the (θ,φ) dependence of the spectrum for $\Psi=10°$ and the same conditions as in Fig. 7 for the lamellar grating.

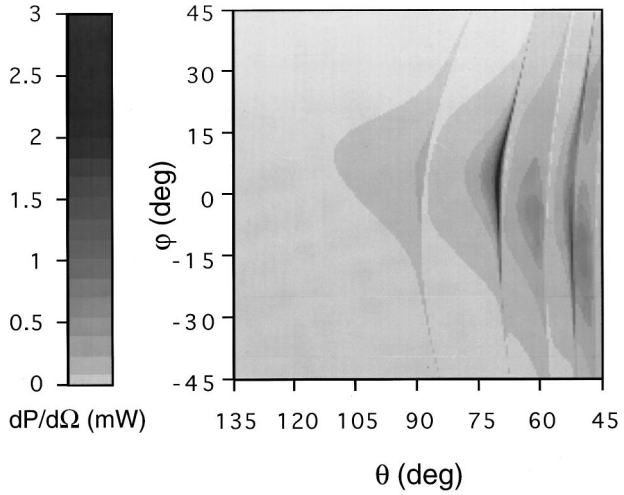

FIG. 8. SP spectrum in first order for a 2-MeV electron beam interacting with a lamellar grating at an incidence angle $\Psi=10°$. Same beam and grating parameters as in Fig. 7. The electron passes over the grating from left to right.

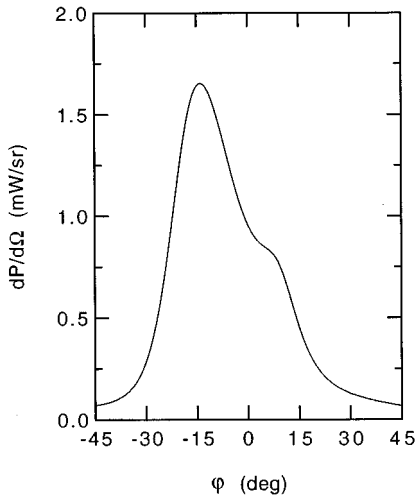

FIG. 9. SP spectrum in first order as a function of the azimuthal angle φ for a 2-MeV electron beam interacting with a lamellar grating at an incidence angle $\Psi=10°$. Same beam and grating parameters as in Figs. 7 and 8. The observation angle $\theta=52.5°$ is close to the $|n_{\max}|=5$ Wood-Rayleigh anomaly.

Contrary to SP radiation produced by electrons moving perpendicular to the rulings, the emission pattern is not symmetrical with respect to the angle φ. The maxima in the spectral distribution reflect the (θ,φ) relation of the Wood-Rayleigh anomalies given by Eqs. (34)–(37). In Fig. 9 we show the φ dependence of the spectrum at $\theta=52.5°$ ($\lambda=0.419$ mm) before and close to the $|n_{\max}|=5$ Wood-Rayleigh anomaly for the same lamellar grating and electron beam as in Fig. 8. The emission is strongly asymmetric with respect to the electron beam trajectory and maximum emission occurs in this case at an azimuthal angle $\varphi\approx-12°$.

VI. CONCLUSIONS

We have calculated SP radiation produced by an electron moving parallel to a grating at arbitrary angles with respect to the rulings. The SP effect has been treated as a special case of conical diffraction by a grating, when the incident electromagnetic field is evanescent. The radiation factor—equivalent to the diffraction coefficients—was calculated applying techniques from the electromagnetic theory of gratings. The diffraction law and a general expression for the SP power emitted by a single electron moving over the grating have been derived. Relations to check the validity of the numerical solutions of the SP grating problem have been given. Tilting the grating with respect to the electron beam trajectory offers a convenient way of fine tuning the wavelength of the emitted radiation. By generalizing this theory for coherent radiation, it could be applied to the study of orotron configurations. However the optimization of experiments using SP radiation at oblique incidence involves careful computation of the spectral-angular distribution taking into consideration the position of the Wood-Rayleigh anomalies.

ACKNOWLEDGEMENTS

One of us (O.H.) gratefully acknowledges the help of J. Harthong and Y. Takakura on several mathematical problems, and for valuable theoretical remarks and suggestions.

[1] S. J. Smith and E. M. Purcell, Phys. Rev. **92**, 1069 (1953).
[2] P. A. Cherenkov, Dok. Akad. Nauk. SSSR **2**, 451 (1937).
[3] S. I. Vavilov, Dok. Akad. Nauk. SSSR **2**, 457 (1937).
[4] I. E. Tamm and I. M. Frank, Dok. Akad. Nauk. SSSR **14**, 107 (1937).
[5] I. Tamm and V. L. Ginzburg, J. Phys. (USSR) **9**, 353 (1945).
[6] V. L. Ginzburg and I. Tamm, Zh. Eksp. Teor. Fiz. **16**, 15 (1946).
[7] B. M. Bolotovskii and G. V. Voskresenskii, Usp. Fiz. Nauk. **88**, 209 (1966) [Sov. Phys. Usp. **9**, 73 (1966)].
[8] P. M. van den Berg and A. J. A. Nicia, J. Phys. A **9**, 1133 (1976).
[9] G. Toraldo di Francia, Nuovo Cimento **16**, 1065 (1961).
[10] *Electromagnetic Theory of Gratings*, edited by R. Petit (Springer-Verlag, Berlin, 1980).
[11] O. Haeberlé, P. Rullhusen, J.-M. Salomé, and N. Maene, Phys. Rev. E **49**, 3340 (1994).
[12] J. P. Bachheimer and J.-L. Bret, C. R. Acad. Sci. Paris Ser. B **266**, 902 (1968).
[13] J. P. Bachheimer, Phys. Rev. B **6**, 2985 (1972).
[14] A. Gover, P. Dvorkis, and U. Elisha, J. Opt. Soc. Am. B **1**, 723 (1984).
[15] I. Shih *et al.*, J. Opt. Soc. Am. B **7**, 345 (1990).
[16] G. Doucas *et al.*, Phys. Rev. Lett. **69**, 1761 (1992).
[17] K. J. Woods *et al.*, Phys. Rev. Lett. **74**, 3808 (1995).
[18] K. Ishi *et al.*, Phys. Rev. E **51**, R5212 (1995).
[19] Y. Ishibata *et al.*, in *Proceedings of the 2nd International Symposium on Radiation of Relativistic Electrons in Periodical*

Structures RREPS 95, edited by Yu. L. Pivovarov and A. P. Potylitsin (Cambridge Interscience, Cambridge, 1996).
[20] J. M. Wachtel, J. Appl. Phys. **50**, 49 (1979).
[21] R. P. Leavitt, D. E. Wortman, and H. Dropkin, IEEE J. Quantum Electron. **QE-17**, 1341 (1981).
[22] D. E. Wortmann and R. P. Leavitt, in *Infrared and Millimeter Waves*, edited by K. J. Button (Academic, New York, 1983), Vol. 7, p. 321.
[23] L. Schächter and A. Ron, Phys. Rev. A **40**, 876 (1989).
[24] F. S. Rusin and G. D. Bogomolov, Proc. IEEE **57**, 720 (1969).
[25] J. P. Bachheimer, Ph.D. thesis, Grenoble, 1971 (unpublished).
[26] E. L. Burdette and G. H. Hughes, Phys. Rev. A **14**, 1766 (1976).
[27] P. M. van den Berg, J. Opt. Soc. Am. **63**, 1588 (1973).
[28] R. W. Wood, Philos. Mag. **4**, 396 (1902).
[29] J. W. S. Rayleigh, Philos. Mag. **14**, 60 (1907).
[30] A. Hessel, Can. J. Phys. **42**, 1195 (1964).
[31] In the corresponding formulas for $\Psi=0°$ published in [11,14] a factor of $n^2/2$ is missing.
[32] L. N. Deryugin, Radiotekh. Elektron. **15**, 9 (1996) [Radio. Eng. Electron. Phys. (USSR) **15**, 12 (1960)].
[33] L. N. Deryugin, Radiotekh. Elektron. **15**, 15 (1960) [Radio. Eng. Electron. Phys. (USSR) **15**, 25 (1960)].
[34] J. W. S. Rayleigh, Proc. R. Soc. London Ser. A **79**, 399 (1907).
[35] R. F. Millar, Proc. Cambridge Philos. Soc. **65**, 773 (1969).